International Journal of Refractory Metals & Hard Materials 82 (2019) 69–80

Contents lists available at ScienceDirect

International Journal of Refractory Metals & Hard Materials

journal homepage: www.elsevier.com/locate/IJRMHM

An overview of creep in tungsten and its alloys

J. Webb[a], S. Gollapudi[b,*], I. Charit[a]

[a] Chemical and Materials Engineering, University of Idaho, Moscow, ID, USA
[b] School of Minerals, Metallurgical, Materials Engineering, IIT, Bhubaneswar, India

A B S T R A C T

The objective of this short review is to provide an overview on the current understanding of creep in tungsten and its alloys. Tungsten is a high temperature material on account of its high melting point and has been historically used for light bulb filaments. In recent years it has been under active consideration for plasma facing liners; an application that demands high temperature strength and durability wherein creep performance becomes important. However, tungsten suffers from poor formability which causes difficulties in making complex parts and components from it. A lot of work has been conducted to improve the formability of tungsten and factors such as amount of cold work, alloying additions and grain size and shape were found to play an important role in improving formability of tungsten. Contrary to conventional metals, the ductility of tungsten is enhanced with increasing cold work. Since recrystallization leads to creation of strain-free grains, and recrystallization is a high temperature phenomena, the ductility of tungsten is intricately related to its ability to resist recrystallization to as high temperatures as possible. Since high temperatures invariably make the role of creep deformation important, a lot of work has been carried out to understand the influence of the ductility-enhancing factors on creep of tungsten and its alloys. The review discusses the role of different factors such as grain size and grain shape, rhenium concentration, potassium as dopant, dispersion strengthening with HfC, ThO_2, La_2O_3 and effect of oxygen containing environment on the creep behaviour of tungsten. Wherever possible, data from literature was analyzed to extract important creep parameters such as stress exponent, grain size exponent, activation energy and Larson-Miller parameter to gain an understanding of the mechanism of creep deformation in tungsten and its alloys. It was observed that fine grain size, low rhenium concentration, high potassium content, addition of dispersions especially of HfC, low oxygen concentration and oblong shaped grains are all beneficial for high creep resistance of tungsten.

1. Introduction

Tungsten is a high temperature material with a melting point of 3695 K, the highest of any metals. Due to its high melting point, it becomes a material of choice for applications involving high service temperatures [1–3]. The use of tungsten for incandescent bulb filaments is one known example where the brightness of the bulb depends on the temperature of operation of the filament. Tungsten is also under consideration as plasma facing liner material for the fusion reactors [4,5].

Fusion reactors are envisioned to provide clean and limitless energy and the ITER project has been at the forefront to demonstrate the viability of producing net gain in fusion energy for extended periods of time using the tokamak [6]. The tokamak is a magneto-fusion device developed to confine the gaseous plasma produced upon the initiation of the fusion reaction. Although the plasma produced inside the tokamak will be controlled and confined using strong magnetic fields, the walls of the vessel confining the plasma will nevertheless be exposed to high temperatures and hence must be constructed out of materials which are capable of sustaining the plasma temperatures without degradation. Fig. 1 shows the cross-section of the tokamak under use in the ITER project and as the figure demonstrates primarily three materials i.e. tungsten, carbon and beryllium are under active consideration for making the plasma facing components [7].

Duffy [7] discusses the expected characteristics of the materials to be used for the plasma facing application. The plasma facing materials are not only expected to protect the walls of the tokamak vessel from high particle flux but also should conduct the high thermal energy. Hence the plasma facing materials are required to bear high thermal conductivity and high sputtering resistance. The choice of material lining the walls is also guided by their tendency to cause radiative cooling of plasma. The plasma lining material must typically bear a low atomic number so that the sputtered atoms have a lower cooling penalty on the plasma.

Generally carbon has the combination of low atomic number, high thermal conductivity and high melting point necessary for the plasma facing application. However carbon has a high susceptibility to hydrogen sputtering and also causes a high tritium inventory and as a result metal liners are preferred over carbon. Despite the high atomic number of tungsten and the associated issues with plasma radiative cooling, tungsten liners are preferred over carbon liners on account of its high sputtering resistance and lower tritium inventory. Tungsten has a high energy threshold for physical sputtering $E_{th} \sim 200$ eV for Deuterium and does not easily form hydrides on interaction with the gaseous plasma. Tungsten also bears very good thermal conductivity

* Corresponding author.
E-mail address: srikantg@iitbbs.ac.in (S. Gollapudi).

https://doi.org/10.1016/j.ijrmhm.2019.03.022
Received 5 February 2019; Received in revised form 21 March 2019; Accepted 30 March 2019
Available online 01 April 2019
0263-4368/

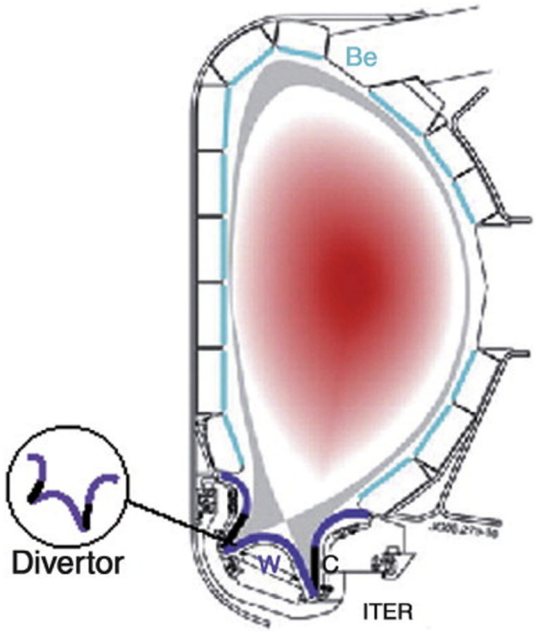

Fig. 1. The cross section of the tokamak for the ITER project. Tungsten and Carbon are under consideration as plasma facing material for the construction of the divertor [7].

and high temperature strength. This attractive portfolio of properties renders tungsten suitable for the plasma facing application in the ITER project. Several studies have been conducted in recent years to discuss the effect of plasma interaction on the properties or surface characteristics of tungsten and its alloys [8–14].

Although tungsten has an attractive combination of properties, it suffers from poor formability despite being a bcc metal like iron. Tungsten has a bcc crystal structure and unlike other bcc metals, like iron, it is not readily formable [15,16]. Tungsten provides low ductility and peculiarly the ductility of annealed tungsten is lower compared to that of cold worked tungsten. Conventionally metals display higher ductility in annealed condition compared to a cold worked condition and the behaviour of tungsten in that context has been a subject of several reviews. Review of the existing literature suggests that the grain morphology as well as the tendency of impurities to segregate at the grain boundaries are controlling factors in the ductility of tungsten [15,16]. In their review, Ren et al. [16] discussed different methods for improvement of ductility of tungsten. As mentioned earlier, thermomechanical processing is an accepted approach for improving ductility. The thermomechanical processing not only improves the dislocation density but also creates pancake shaped grains which are apparently beneficial from a ductility standpoint. Work by different groups [17,18] has shown that thermomechanical processing at 673 K leads to significant improvement in ductility of tungsten. The deformed tungsten was found to bear a significant fraction of low angle grain boundaries and increased dislocation density.

The anomalous deformation behaviour of tungsten is also observed in its response to alloying element additions. Generally the addition of alloying elements leads to strengthening of metals [19] albeit at the loss of some ductility [20]. However in the case of tungsten the addition of rhenium not only causes softening but also improves its ductility [21]. Apparently rhenium reduces the Peierls stress and also promotes the operation of {112} slip planes during plastic deformation which leads to the improvement in ductility. The effect of other alloying elements such as Ti, Mo, Ta, Ir, Zr, K etc. on the ductility of tungsten has also been investigated. Among all these different elements, Ir has provided results similar to that of Re [22,23] but tungsten alloy development based on Ir additions will be an expensive affair and hence did not gain significant traction.

Improvement in ductility through grain size refinement has also been attempted and it has been observed that ductility improvement is achieved through the top-down approach with no conclusive reports on the bottom-up approach [24–26]. Herein it is important to note that there is still some ambiguity on if the improvements are entirely due to grain size refinement or if there is a role of the increased dislocation density brought about by the refinement process.

The ductility and thus the toughness of tungsten and its alloys brought about by thermomechanical processing can be retained as long as the material does not recrystallize as recrystallization will lead to the creation of strain free grains and reduce the dislocation density of the material [27,28]. Hence a key aspect of alloy development is increasing the recrystallization temperature of tungsten and its alloys. Increasing the recrystallization temperature leads to the following benefits a. Increases the thermomechanical processing window of tungsten b. Increases the service operation window of tungsten without the risk of recrystallization. Although mechanical working improves the formability of tungsten it also leads to reduction in the recrystallization temperature. It is well known and widely accepted that higher the degree of cold work, lower is the recrystallization temperature [29]. Since recrystallization will lead to loss of ductility of tungsten, efforts have been directed at increasing the recrystallization temperature. The mechanism of recrystallization is usually discussed in terms of migration of a high angle grain boundary that sweeps/cleans the high dislocation content of the cold worked grains. Hence introducing barriers to the motion of the high angle grain boundary can lead to enhancement in the recrystallization temperature. Weseman et al. [30] and Chen et al. [31] have demonstrated that the addition of elongated La_2O_3 to the tungsten microstructure enhances the recrystallization temperature.

In a recent study, Zhang et al. [32] investigated the effect of degree of deformation on the recrystallization behaviour of pure W and W-La_2O_3 alloy produced by powder metallurgy route. Interestingly, Zhang et al. [32] found that the recrystallization temperature increased with increasing deformation. The increase in recrystallization temperature was attributed to the improved performance of La_2O_3 in inhibiting the migration of the high angle grain boundaries following mechanical working. Although the improvement in performance was attributed to the elongation of La_2O_3 particles, a possible cause could also be the breaking of La_2O_3 particles into finer sizes leading to more uniform distribution of these particles and consequently greater barrier to boundary migration. Zhang et al. [32] observed an improvement in recrystallization temperature by almost 300 K of the W-La_2O_3 material compared to pure W.

Based on the discussion so far, it is clear that three broad approaches have been adopted for the improvement of ductility in tungsten a. thermomechanical processing b. alloying or second phase additions, and c. grain size refinement. Also in order to retain the ductility, efforts have been directed to increase the recrystallization temperature of tungsten.

Although the focus of our review is on creep of tungsten and its alloys, it is important to discuss ductility of tungsten and the factors controlling the same. Since the formability of components based on tungsten and its alloys will be controlled by the different factors influencing ductility, it is of interest to understand these factors and consequently their effect whatsoever on the creep behaviour of tungsten and its alloys.

High temperature operating conditions invariably bring in the role of creep plastic deformation. Creep is defined as the time dependent plastic deformation of a material and can contribute to the premature failure of a component during service if it is not accounted for and preemptory steps are not taken. A comprehensive understanding of the mechanisms of creep and their contribution towards creep deformation for a certain combination of operating conditions, especially applied loads and service temperature, is required for the design of a component from a certain material. Although the mechanical properties of

tungsten such as strength and ductility have been regularly studied as well as reviewed [33,34], there are not many studies addressing the creep performance of tungsten and its alloys. The objective of the current article is to conduct a review of existing literature on the creep behaviour of tungsten and its alloys and also draw conclusions from the available data by analysing the Larson-Miller parameters and deformation mechanism maps.

In our review, discussion on the creep behaviour of tungsten and its alloys has been divided into two sections. The first section is dedicated to understanding the creep behaviour of nominally pure tungsten and the second section is dedicated to understanding the creep of tungsten alloys which includes doped tungsten as well as dispersion strengthened tungsten. The objective of separating the review into two sections is that it allows a better appreciation of the effect of alloying/dopant/dispersion additions on the creep performance of tungsten.

2. Section I: creep of nominally pure tungsten

Creep is traditionally thought of as a high temperature, time dependent plastic deformation of a material under the influence of applied stress or load. Time dependent creep is commonly broken down into three distinct regimes. Stage I or primary creep (ε_p) is characterized by a decreasing strain rate of deformation brought by about by a competition between strain hardening and recovery mechanisms. During the primary creep stage, the material experiences an evolution of the dislocation substructure. The Stage II creep, also known as steady state or linear creep ($\dot{\varepsilon_{ss}}$) begins when an equilibrium is achieved between mechanisms of strain hardening and recovery and is characterized by a constant strain rate of deformation. Stage III creep, better known as tertiary creep (ε_{tc}) is characterized by an increasing strain rate of deformation and can be identified by a rapid increase in the slope of strain vs. time, eventually leading to specimen failure. Fig. 2 shows a plot of strain vs. time for arc-melted tungsten at varying levels of applied stress and temperature [35].

Steady state creep is usually the most heavily analyzed portion of the creep curve. Many relationships have been developed to explain steady state creep [35–42]; however, most of them view creep as a process based on dislocation climb. The preferred relationship that relates the creep rate ($\dot{\varepsilon}_{ss}$) with the Burgers vector (b), average grain size (d), diffusion coefficient (D), Young's modulus (E), applied stress (σ), temperature (T), Boltzmann's constant (k), grain size exponent (p) and stress exponent (n) is shown in Eq. (1).

$$\dot{\varepsilon}_{ss} = A\left(\frac{b}{d}\right)^{p}\left(\frac{D\,E\,b}{kT}\right)\left(\frac{\sigma}{E}\right)^{n} \tag{1}$$

Within Eq. (1), the term A represents a magnitude factor that is usually derived empirically and the diffusion coefficient (D) is also empirically derived and related to a specific mechanisms. It used to be thought that creep only occurred at temperatures that ranged from $0.5T_m$ to $0.75T_m$; however, experiments have shown creep behavior at temperatures as low as $0.3T_m$ [43–45]. Multiple experiments have been conducted to determine the activation energy of tungsten for creep over the temperature range of $0.3T_m$ to $0.9T_m$, all of which seem to indicate a large drop in the activation energy at an approximate value of 2200 K. ($0.6T_m$) [35–37,44,46–49]. Above 2200 K, the activation energy extrapolated from an Arrhenius relationship indicates an activation energy that ranges from 525 kJ/mol to 620 kJ/mol. Below 2200 K, the extrapolated activation energy ranges from 368 kJ/mol to 460 kJ/mol. Fig. 3 shows a plot of data points compiled by the authors of this study indicating the extrapolated activation energy as a function of temperature from 4 different references [46–49].

The high temperature creep activation energy has been correlated to lattice diffusion which has an activation energy of 520 kJ/mol as measured by tracer diffusion experiments [50–53]. However, the drop in activation energy below 2200 K is still a matter of much debate. The prevailing theory involves vacancy migration along short-circuiting dislocation cores allowing for edge dislocation climb, leading to a dislocation-core diffusion activation energy of 385 kJ/mol, which also happens to closely correspond with the activation energy for grain boundary diffusion [54,55]. However, dislocation cross-slip and obstacle controlled glide processes have also been offered as competing theories [41]. The debate over low temperature creep mechanisms is still a matter of discussion; however, the measured activation energies seem to indicate that from $0.3T_m$ to $0.6T_m$, the creep mechanism is associated with dislocation-core diffusion.

2.1. Power law relationship

The steady state creep rate of most class M metals can be described as a power law relationship as shown in Eq. (1), where n represents the power-law exponent that usually takes on a value of 5. Robinson and Sherby previously compiled many experimental results from different authors to determine the value of n for tungsten [44]. The diffusion coefficient shown in Eq. (1) is usually assumed to be the lattice diffusion coefficient; however, Robinson and Sherby [44] assumed that at low temperatures, dislocation-core diffusion also played a role in the

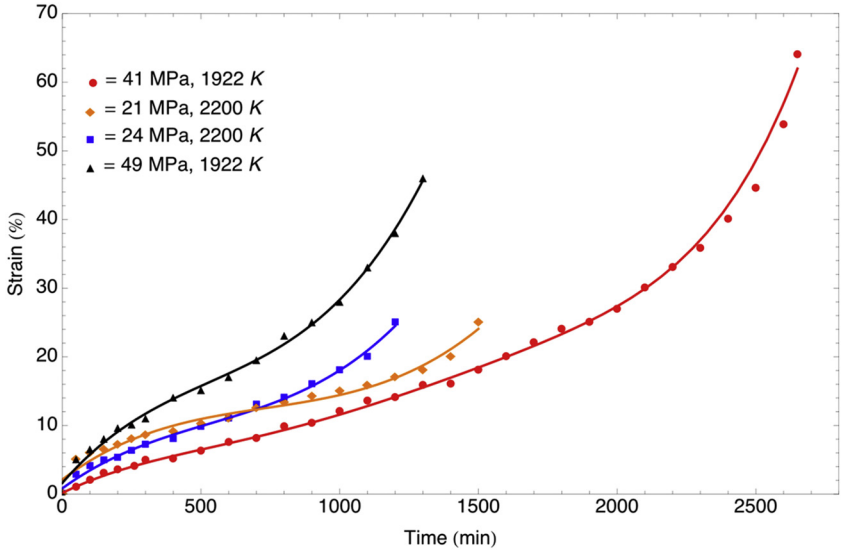

Fig. 2. Plot of strain versus time for arc-melted tungsten in tension.

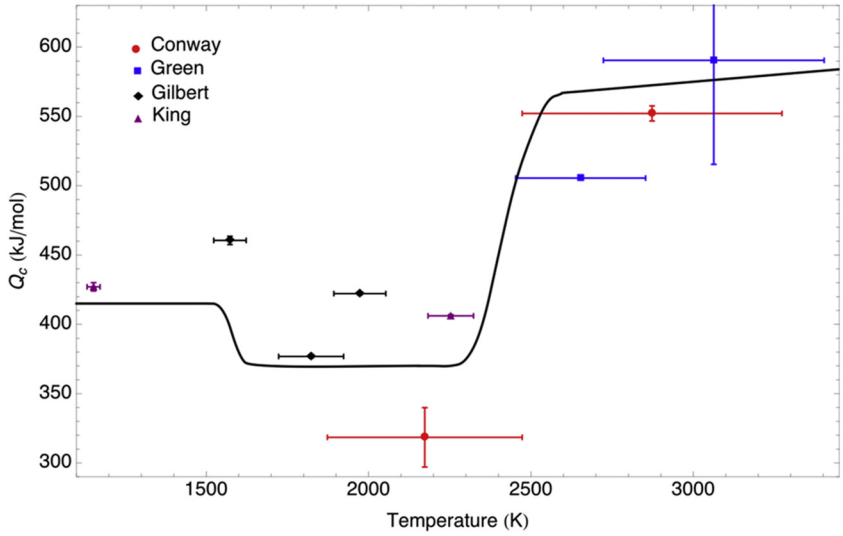

Fig. 3. Plot of extrapolated creep activation energies for tungsten as a function of temperature.

creep deformation process. Robinson and Sherby [44] developed an effective diffusion coefficient with pre-exponential frequency factors based on the number atom sites that play a role in each of the individual processes, as opposed to the traditional pre-exponential frequency factors. The measured steady state creep rates were divided by the effective diffusion coefficient which was then plotted against the modulus compensated stress (σ/E). The slope of the trend was then determined as the value of the power law stress exponent n.

The study conducted by Robinson and Sherby [44] concluded that tungsten fabricated by arc-melting and electron-beam-melting techniques had a power-law exponent of 5, and the power law exponent of powder metallurgy tungsten was found to be approximately 7. They also concluded that the value of n was dependent on the number of subgrains present prior to and during creep testing. However, recent studies seem to indicate that subgrains may be the effect of creep, not the cause of the relationship. It also appears that Robinson and Sherby [44] plotted data for both fully recrystallized tungsten as well as wrought tungsten, which would have likely affected the results.

Data from six historical experiments were compiled and analyzed based on modern creep theories to determine the value of power-law exponent. Two experiments were conducted by NASA-LeRC [35–37] where arc-melted and electron-beam-melted tungsten specimens were tested at applied stresses ranging from 15 MPa to 77 MPa over a temperature range of 1500 K to 2400 K. The NASA data were compiled from fully recrystallized tungsten with average grain diameters ranging from 70 μm to 4000 μm. Data was also collected from studies of Flagella and Conway [49] where fully recrystallized tungsten fabricated by arc-melting techniques was tested over a range of 1800 K to 3300 K and 2 to 70 MPa. The average grain size of specimens tested by Flagella and Conway is unknown. The next data set was collected from Green's work [47] over the temperature range of 2523 K to 3100 K and applied stress values of 9 to 50 MPa. The specimens tested by Green were fabricated by powder metallurgy techniques and had a fine microstructure with an average grain size of approximately 10 μm. Another series of experiments were conducted by King and Sell [46] on powder metallurgy specimens from 1200 K to 2700 K and applied stress values as high as 200 MPa. The specimens had an average grain size of 40 μm. Finally data was also collected from Harris and Ellison [48] where wrought powder metallurgy tungsten was tested at temperatures ranging from 1000 K to 1500 K under stresses from 150 MPa to 700 MPa.

The creep data expressed in the form of $\dot{\varepsilon}\, kT/D_{eff}\, E\, b$ are plotted for each of the data points vs. σ/E. The value of effective diffusion coefficient (D_{eff}) was determined from the sum of the pre-exponential frequency factors and activation energies for dislocation-core diffusion and lattice diffusion in tungsten. Dislocation-core diffusion has an activation energy similar to the activation energy for grain boundary diffusion due to the fact that grain boundaries can be described as an array of dislocations. However, the pre-exponential frequency factor for dislocation-core diffusion has never been measured. Prior experiments have confirmed that the contribution from lattice diffusion becomes the dominant mechanisms for power-law creep at an approximate temperature of 2200 K. With knowledge of the activation energies for both mechanisms, the pre-exponential frequency factor for lattice diffusion and the cross-over temperature, the pre-exponential frequency factor for dislocation-core diffusion can be analytically determined. The relationship describing the effective diffusion coefficient is shown in Eq. (2), where the pre-exponential frequency factors ($D_{dc}{}^{o}$) and ($D_{l}{}^{o}$) are $9.22 \times 10^{-9}\,m^2/s$ and $8 \times 10^{-6}\,m^2/s$ respectively.

$$D_{eff} = D_{dc}^{o} e^{-\frac{Q_{dc}}{RT}} + D_{l}^{o} e^{-\frac{Q_{l}}{RT}} \tag{2}$$

The values of activation energy in Eq. (2) for Q_{dc} and Q_l are 385 kJ/mol and 520 kJ/mol respectively. While Eq. (2) was determined partially from empirical and analytical data, the results match very closely with a purely analytical technique first proposed by Ashy and Frost in 1983 [56].

All of the data sets with exception to Green's [47] and Harris's [48] fell very neatly onto a single trend curve in Fig. 4. The data set produced by Harris and Ellison [48] was based on wrought tungsten and as such it was not expected to follow the same power-law trend. The data provided by Green [47] followed the same power-law trend; however, Green's data was found to have an unusually low magnitude on the curve. It is not clear why the data provided by Green did not have the same magnitude as other data points, other than the fact that the average grain size was much smaller than that tested in other studies. The effects of microstructure on the creep properties of tungsten will be further discussed in the next section; however, it is sufficient to say that the linear creep rate of tungsten appears to decrease as the average grain size decreases, which may explain the lower magnitude of Green's data. The data trends all seem to have the same power-law exponent of 4.2, which is shown in Fig. 4. This recent analysis also seems to indicate little difference between powder metallurgy tungsten and arc/electron-beam-melted tungsten, which is against the suggestions of Sherby and Robinson [44]. Tungsten produced from both fabrication techniques seem to have the same power-law exponent (n) and they both begin to undergo power law breakdown at a $\dot{\varepsilon}\, kT/D_{eff}\, E\, b$ of 10^{-6}, which compares well against other class M-type metals [41]. Finally, it is important to note that the wrought tungsten tested by Harris and Ellison

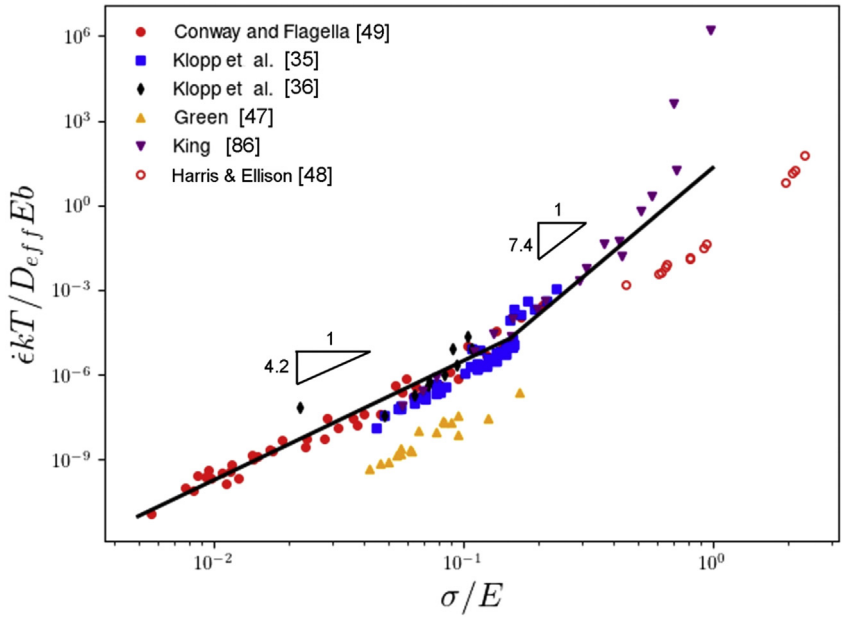

Fig. 4. Power-law relationship for steady state creep rates for recrystallized and wrought tungsten.

[48] maintains a traditional power-law relationship at very high values of σ/E, indicating that the subgrain walls that were present in the wrought tungsten might have delayed the onset of power-law breakdown.

2.2. Creep-grain size relationship

The linear creep rate of most metals decreases as the average grain size increases. The time to rupture is also usually proportional to the average grain size for most class M metals. The observed linear creep rate for tungsten does not follow the traditional trend held by most class M metals and alloys. The review of literature seems to indicate that the creep rate for tungsten decreases with decreasing grain size and that the time to rupture also increases with decreasing grain size.

Robinson and Sherby [44] proposed that the creep rate within tungsten is proportional to the areas swept out by dislocations from creation to annihilation. They also postulated that within tungsten, the grain boundaries and subgrain boundaries serve as sink sites for the annihilation of dislocations, indicating that the creep rate should be proportional to the square of the average grain diameter. A study of NASA-LeRC [57] investigated the linear creep rate of powder metallurgy tungsten with average grain sizes ranging from 30 to 3000 μm. Eq. 1 predicts a relationship between the linear creep rate ($\dot{\varepsilon}_{ss}$) and the grain size exponent (p). The data from the NASA-LeRC study was fitted to determine the value of p, which was determined to be −1.75, which is very close to the value of 2 predicted by Robinson and Sherby; however, the sign is inverted indicating a behavior opposite of most class M metals. Fig. 5 shows a plot of $\dot{\varepsilon}\, d^{1.75}$ vs. σ/E where the relationship between grain size and creep rate is clearly demonstrated. It is also important to note that the slope of the trend plotted in Fig. 5 is 4.2, which is equal to the power-law exponent of 4.2, further lending credibility to the relationship between grain size and creep rate.

The data points collected for this research was empirically fitted to determine the value of A and n for the regions of 5 PLC and 7 PLC. For the 5 PLC region which was found to occur below a σ/E ratio of 0.16, the values of A and n were found to be $1.51 \times 10^{-12}\,s^{-1}$ and 4.2 respectively, where above a modulus compensated value of 0.16, the values were found to be $5.54 \times 10^{-10}\,s^{-1}$ and 7.4 respectively. Eq. (1) can now be re-written in the form of Eq. (3) to yield a final linear creep rate relationship for tungsten where all terms are entered in the SI units of meters, Kelvins and seconds. Notice that the parameter b/d was re-written as d/b in order to keep the exponent p as a positive number, which indicates a proportional relationship between the grain size and creep rate which is unusual for class M metals.

$$\dot{\varepsilon}_{ss} = A\left(\frac{d}{b}\right)^{1.75}\left(\frac{D_{eff}Eb}{kT}\right)\left(\frac{\sigma}{E}\right)^{n} \tag{3}$$

2.3. Rupture

At some point during the creep process, voids are created and grow coalesce in the triple points. Following this the material enters stage III or tertiary creep. Tertiary creep is characterized by a marked increase in the slope of strain vs. time and ends with specimen failure. The time to rupture/failure (t) can be related to the applied stress by the Larson-Miller parameter (Z), which is shown in Eq. (4), where C is a material dependent parameter.

$$Z = T\,[C + Log(t)] \times 10^{-3} \tag{4}$$

The rupture life data from the work of Klopp, Green, Harris and Flagella [35–37,46–49] were used to determine the value of C as well as a stress dependent relationship for Z. The data presented by Klopp et al., as well as Flagella and Conway [49], relates the time to rupture for arc/electron beam melted tungsten and the rest of the data described the time to rupture for powder metallurgy tungsten. The data clearly showed that powder metallurgy tungsten has a longer time to rupture than arc/electron beam melted tungsten. The increase in rupture time is likely due to the finer microstructure obtained from powder metallurgy tungsten that acts as dislocation barriers. The value of C was fit to ~12.3 for arc and electron beam melted tungsten and ~11.5 for powder metallurgy tungsten. Fig. 6 shows a plot of the Larson-Miller parameter vs. stress.

The values of Z were also fitted to a logarithmic relationship shown in Eq. 9 for both powder metallurgy tungsten and arc/electron-beam melted tungsten. Within Eq. 5, the appropriate values of C must be input for the two fabrication techniques.

$$56.24\sigma^{-0.191} = T\,[C + Log(t)] \times 10^{-3} \tag{5}$$

2.3.1. Deformation mechanism maps

Three dominant creep mechanisms exist by which a material deform at high homologous temperatures. Power-law creep is a dislocation-

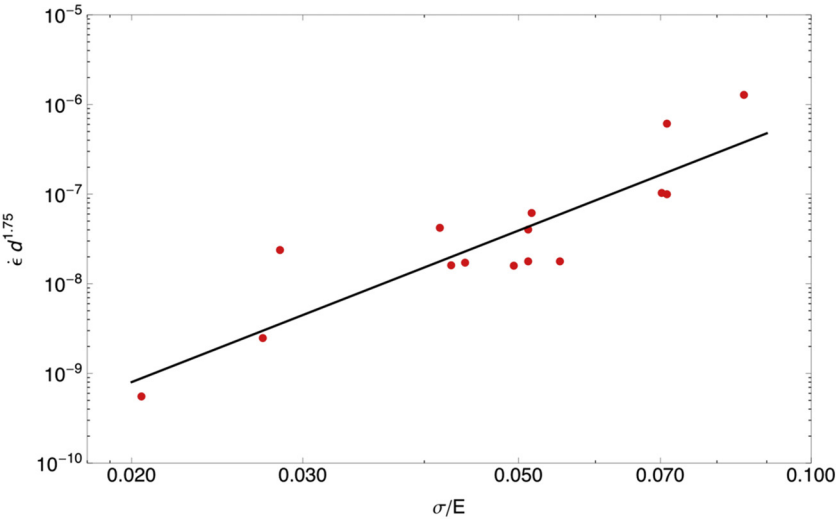

Fig. 5. Plot of the steady state creep rate ($\dot{\varepsilon}$) multiplied by the grain size (d) raised to the\ 1.75 power vs. modulus compensated stress (σ/E).

climb-based mechanism by which a material deforms and usually require a higher stress. Coble creep is another low stress mechanism by which a material can be deformed and is purely diffusional in nature. Coble creep occurs, by the diffusion of atoms through vacancies within the grain boundaries of a material and as such is based on grain boundary diffusion. Finally, Nabarro-Herring creep is another diffusion-based mechanism. Nabarro-Herring creep is based diffusion of atoms through vacancy mechanism within the lattice structure and is controlled by lattice diffusion. The relationships for steady state Coble and Nabarro-Herring creep rates are shown in Eqs. 6 and 7, respectively [58].

$$\dot{\varepsilon} = 7.5\frac{b\Omega D_b^0 e^{-\frac{Q_b}{RT}}}{d^3 kT}\sigma \tag{6}$$

$$\dot{\varepsilon} = 40\frac{\Omega D_l^0 e^{-\frac{Q_l}{RT}}}{d^2 kT}\sigma \tag{7}$$

The use of deformation mechanism maps was first proposed by Ashby and Frost in 1972 as a method of understanding the mechanical performance of metals [56,59]. The deformation mechanism maps are produced by solving the creep constitutive relationships as a function of temperature and stress and by determining which mechanism produces the highest creep rate. The mechanism found to have the highest creep rate is the dominant mechanism at that temperature and stress, which can be graphically shown on a deformation mechanism map. The map can also overlay the regions of plastic flow which occur at values of stress above the yield stress and failure which occur at higher stresses.

Deformation mechanism maps have been previously produced for tungsten by Ashby and Frost; however, they were produced using analytical power-law creep relationships as opposed to the empirical data used here. Deformation mechanism maps were prepared for grain sizes of 1, 5, 10, 20, 50 and 100 μm at temperatures ranging from 1200 K to 3665 K in increments of 20 K using the parameters shown in Table 1. A FORTRAN program was used to determine the dominant mechanism at each temperature and the value of applied stress at which the mechanism became dominant. Fig. 7 shows the regions dominance for each mechanism as a plot of stress in units of MPa versus temperature in K. At low values of grain size, Coble creep dominates most of the parameter space at stress values below the plastic limit. However, as the grain size begins to increase, power-law creep and Nabarro-

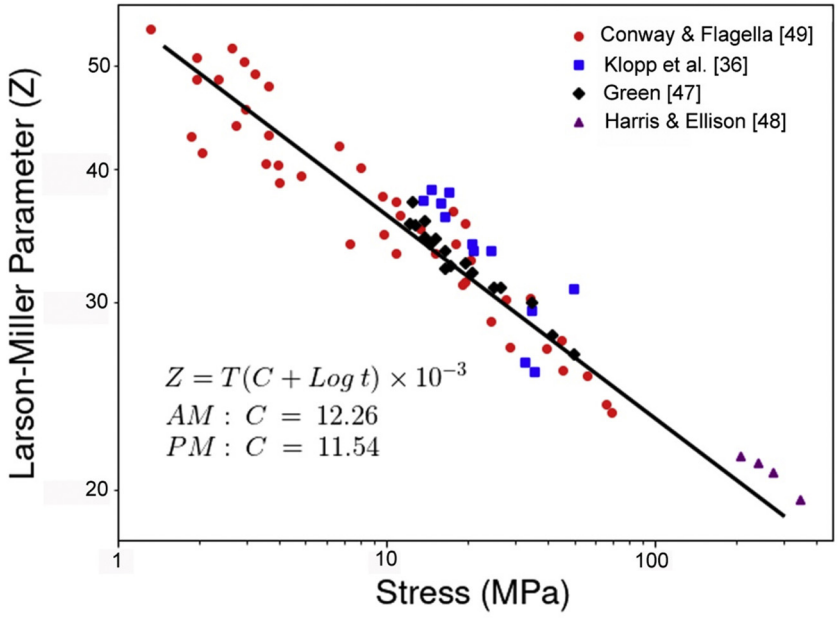

Fig. 6. Larson-Miller relationship for tungsten fabricated by powder metallurgy and arc/electron beam melting techniques.

Table 1
Parameters for development of creep deformation mechanism map of tungsten.

Parameter	Value	Reference
Ω	$1.59 \times 10^{-29}\,m^3$	Frost & Ashby [56] Raj et al. [40]
b	$2.74 \times 10^{-4}\,m$	Frost & Ashby [56]
Q_b	385 kJ/mol	Ashby [60] German [61]
D_b^o	$1.09 \times 10^{-3}\,m^2/s$	Ashby [60] German [61]
Q_l	520 kJ/mol	Krieder & Bruggeman [62] Pawel & Lundy [50]
D_l^o	$8 \times 10^{-6}\,m^2/s$	Krieder & Bruggeman [62]
D_{dc}^o	$9.22 \times 10^{-9}\,m^2/s$	Klopp & Witzke [35] Coble [58]

Herring creep start to inch their way from left to right across the plots. At grain size values around 5, the combination of 5 and 7 power-law creep starts to dominate the plots, and the stress at which plastic flow begins, decreases precipitously. Even at large grain sizes, Nabarro-Herring creep only occurs at relatively low stresses and very high temperatures.

3. Section II: effect of alloying element and second phase additions

The different classes of tungsten based alloys as discussed by Davis [62] are as follows:

- Solid solution alloys containing various amounts of Molybdenum (2 to 20 wt%) or Rhenium (1 to 25 wt%)
- Doped tungsten alloys containing minute quantities of potassium, oxygen, aluminium, silicon etc. The quantities are usually on the order of ppm.
- Dispersion strengthened alloys such as those reinforced with ThO_2 or W—Re alloys with a dispersion of ThO_2 or HfC
- Tungsten heavy alloys including tungsten-nickel-iron, tungsten-nickel-cobalt among others.

Our review on creep will cover only on the first three classes of tungsten alloys. Gallet et al. [63] studied the creep behaviour of tungsten based systems. The creep studies were carried out in the temperature range of 1173–1373 K at applied stress of 10–50 MPa under four point beam testing conditions. The creep tests were carried out on stress relieved tungsten (W-sr), recrystallized tungsten (W-rc), W—B (with Boron at 10, 100 and 205 ppm), W—Re and W—K alloys. Creep tests were also carried out on W-La_2O_3 and a comparison of the creep behaviour of these different systems revealed the following order of creep resistance, ranked from best to worst: W-rc > W-B100ppm > W-La_2O_3 > W-B200ppm > W-sr = W-Re = W-K > W-B10ppm Analysis of the creep data revealed a stress exponent (n) value of 1 and also grain size independence suggested by grain size exponent (p) value of zero. The activation energy of creep, Q_c, was found to be lower than both lattice diffusion activation energy and grain boundary diffusion activation energy. Based on the combination of n and p, the Harper-Dorn creep [64] seems to be the most plausible mechanism controlling the creep of the above mentioned systems for the given test conditions. A stress exponent of 1 is generally associated with Newtonian viscous creep mechanisms such as Nabarro-Herring (N—H) [65,66], Coble creep [67] and Harper-Dorn creep [64]. However, the diffusion creep mechanisms such as N—H and Coble are usually associated with p values of 2 and 3 respectively while $p = 0$ for H-D creep. The operation of H-D creep in the above mentioned systems can also be concluded from the fact that the authors observed dislocation rearrangements in the crept samples and moreover the creep curves revealed significant primary creep region which are generally not associated with N—H and Coble creep.

It is interesting to note that B plays a better role in enhancing the creep resistance of W compared to Re. The reason for the same was not discussed by Gallet et al. [63]. Usually the Boron is in solid solution and the improvement in creep resistance due to Boron addition is mostly due to its pinning effect on dislocations; albeit Raffo and Klopp [68] attribute it to the lowering of grain boundary mobility. A possible reason for the effectiveness of B vis-à-vis Re could be understood by a review of the binary phase diagrams of W—B [69] and W—Re [70]. As the binary phase diagrams suggest, Re has a high solubility in W compared to Boron. Rhenium is probably occupying substitutional sites on account of its atomic radius of 2.05 Angstrom which is not very different from that of Tungsten at 2.1 Angstrom. Furthermore, its elastic modulus at 466 GPa is only mildly higher than that of Tungsten at 411 GPa. On the other hand, Boron has an atomic radius of 1.8 Angstrom and on account of this, Boron in very small quantities could cause higher lattice distortion leading to greater interaction with dislocations and concomitant strengthening.

The effect of Re addition on the tensile creep behaviour of W was studied by Klopp et al. [71] at test temperatures of 3273 K. The minimum creep rate was found to have a power law dependence on the applied stress both for unalloyed tungsten as well as alloyed tungsten. The stress exponents of the different alloys were found to be in the range of 4 to 6 whereas for unalloyed tungsten it was observed to be 5.8. The stress required to achieve a creep rate of $10^{-6}\,s^{-1}$ was determined for the different alloys and it was found that the addition of Re was enhancing the creep resistance of W. However, Re contents of the order of 6–8 wt% were observed to provide a better creep performance than W—Re alloys with Re content in the range of 24 to 26 wt%. This behaviour was in contrast to the room temperature strength of the alloys where the low and high Re containing alloys provide equivalent strength values.

The poor creep performance of the high Re containing W—Re alloys was also observed by Vandervoort [72]. Vandervoort obtained a stress exponent value of 5 from tensile creep studies on W, W-5 wt% Re and W-25 wt% Re and reported higher creep resistance of the W-5 wt%Re alloy compared to the W and W-25 wt% Re alloy. A stress exponent value of 5 is indicative of power law creep with the dislocation climb as the rate controlling mechanism. Interestingly, Vandervoort [72] did not observe the formation of any subgrains during transmission electron microscopy of the post crept samples of W-5 wt% Re. Furthermore, all the W-5 wt% Re samples attained steady state of creep immediately on loading and displayed a very small or negligible primary creep region. The absence of a primary creep region and also the lack of formation of subgrains seems to suggest that the deformation of W—5Re is governed by viscous power law creep. The viscous power law creep is generally associated with a stress exponent of 3 and the microstructures of samples crept in this region generally consist of a random arrangement of dislocations with no particular network [39]. Furthermore, the viscous power law creep is known to occur in solid solutions [73]. As Re is known to dissolve in the W matrix, in all probability the W—5Re material is creeping by viscous power law creep where the deformation is glide-controlled. This conclusion is further validated by the fact that Vandervoort [72] observed the formation of subgrains in the pure W samples crept under similar conditions.

The improvement in creep performance brought about by Re addition was also observed by Gao and Zee [74] who reported that Re in minute quantities increases the activation energy for creep by 28 kJ/mol. A further advantage of Re addition is the increase in recrystallization temperature which is possibly on account of its influence in retarding grain boundary migration. Rhenium additions as low as 1.9 wt% are sufficient to enhance the recrystallization temperature by 873 K.

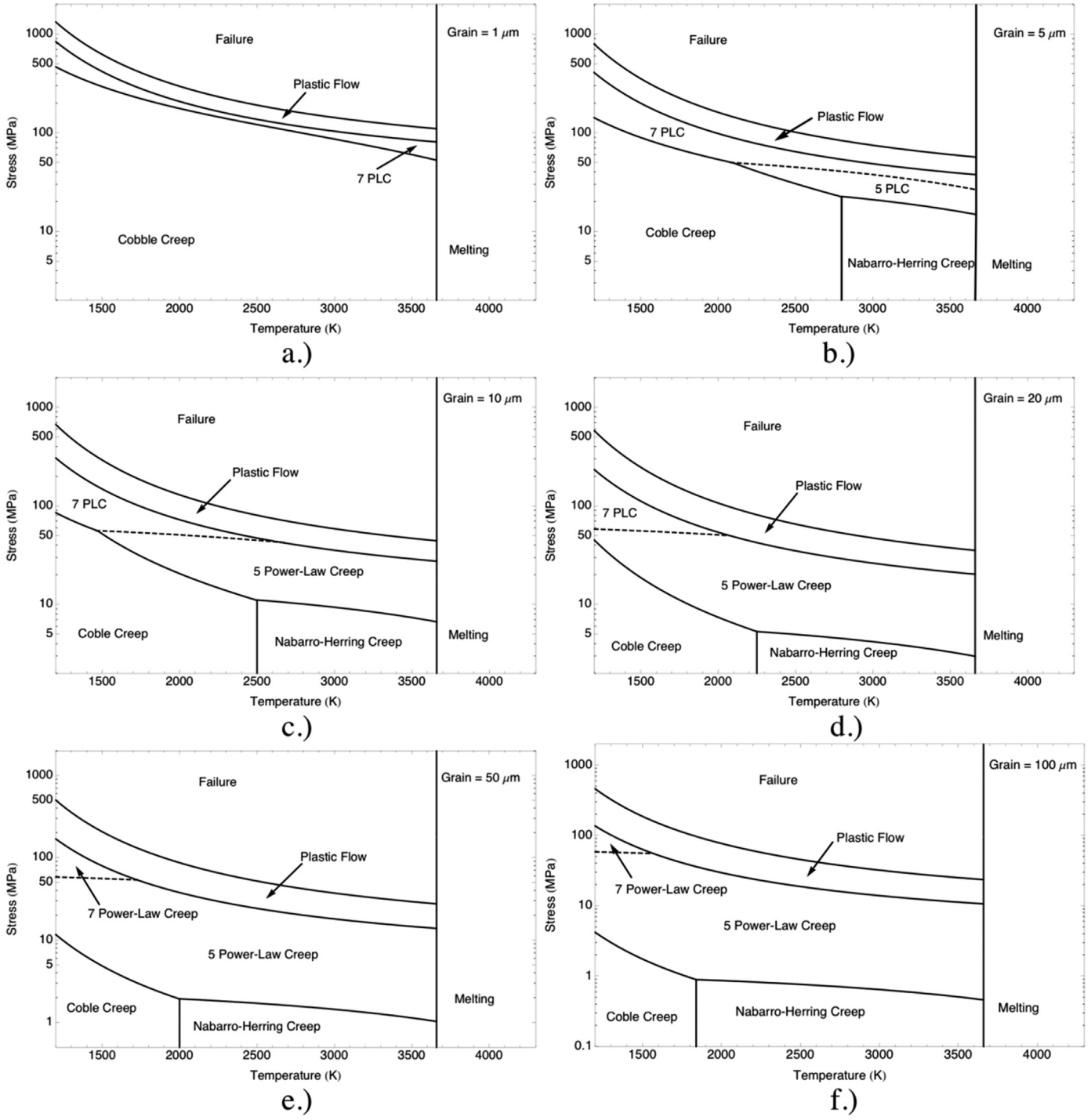

Fig. 7. Creep deformation mechanism maps for tungsten with grain sizes of a) 1 μm, b) 5 μm, c) 10 μm, d) 20 μm, e) 50 μm and f) 100 μm.

3.1. Effect of dopants on creep performance of tungsten

Tungsten is invariably doped with potassium for excellent creep performance for its use as non sag filaments in incandescent bulbs. The addition of potassium leads to the formation of a row of elongated bubbles which creates an interlocking grain structure and renders the material creep resistant [75,76]. The growth of the bubbles is however associated with loss of the creep performance of the tungsten filaments. Studies by Tanoue and Ijichi have shown that the stress exponent of potassium doped tungsten is around 3 for normalized applied stress in the range of 10^{-4} to $10^{-3.5}$ and at higher values, the higher potassium containing tungsten offers greater creep resistance. Increasing the potassium concentration was also found to enhance the hardness of the tungsten grains [77].

The potassium bubbles apparently push the recrystallization temperatures to higher values and this could be on account of the impeding effect of potassium bubbles on the migration of grain boundaries which is necessary for recrystallization. The addition of potassium for stabilization of ultrafine grained structure of tungsten and improvement of high temperature fracture strength has also been the objective of recent studies [2,78,79].

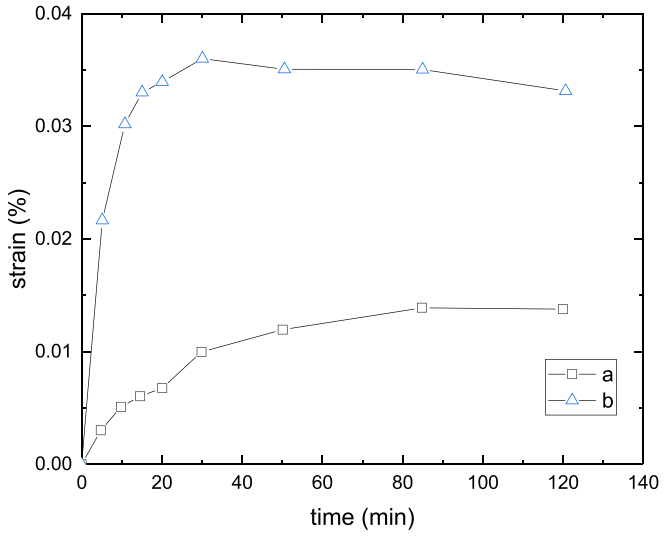

Fig. 8. Effect of tiny quantity of oxygen on the creep of non-sag tungsten. a) creep tests conducted in stagnant argon b. creep tests conducted in oxygen containing argon. Oxygen content was 0.03% [80].

3.2. Effect of oxygen on creep of tungsten

Creep tests were conducted on non-sag tungsten wires to understand the effect of oxygen on the resistance to creep deformation [80]. It was observed that even tiny quantities of oxygen caused significant loss of creep performance. Fig. 8 shows that the creep strain is significantly higher in samples tested in argon with 0.03% Oxygen compared to tests carried out in pure argon. The loss in creep performance was also reflected in the lower activation energy of creep deformation of samples tested in oxygen-containing argon atmosphere. As the figure shows, the activation energy of pure tungsten wires tested in vacuum is 330 kJ/mol and the creep deformation is attributed to grain boundary diffusion whereas Q for tests in oxygen-containing argon is only 90 kJ/mol and the fast diffusion of oxygen in the tungsten matrix was suggested to be the rate controlling mechanism of deformation. The atomic size of oxygen is 1.52 Angstrom whereas that of Tungsten is 2.1 A° and this large atomic size difference is possibly the cause of fast diffusion leading to low activation energies of deformation. Oxygen was also found to increase the size of the potassium bubbles which has a detrimental effect on the non-sag performance of the tungsten filaments [80].

3.3. Creep of dispersion strengthened tungsten alloys

Although the addition of Re renders W ductile, in higher amounts Re compromises the strength and creep resistance of W. In order to address this, studies have been conducted to improve the creep performance of W−Re alloys through the introduction of dispersions of HfC, ThO_2 and other oxides. Work by Witzke [81] showed that the addition of HfC to W−4Re alloy enhanced the strength and creep resistance of the alloy. Arc melted W-4Re-HfC specimens with HfC varying from 0 to 0.8 mol% were evaluated for mechanical properties as well as for ductile-brittle transition temperature (DBTT). Witzke [81] found that the low temperature ductility was independent of the HfC content but rather influenced by the excess Hf and C content above stoichiometric HfC. In fact, the lowest DBTT was obtained for Hf contents slightly in excess of stoichiometry. The rupture life of the alloys was found to be dependent on the HfC content with a maximum in rupture life obtained for HfC contents around 0.35 wt%. Interestingly, Hf contents in excess of the stoichiometry, for a given HfC content, were found to be more beneficial for rupture life in comparison to C contents in excess of stoichiometry. Furthermore, the formation of WC particles

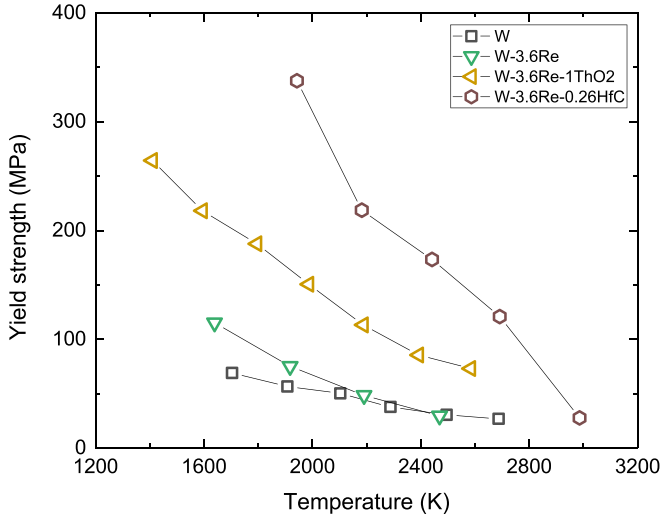

Fig. 9. Effect of Rhenium, Thoria addition and HfC addition on high temperature mechanical properties of W [82].

in the slightly non-stoichiometric compositions of HfC was also found to influence the creep behaviour. It was observed that the minimum creep rate increased with the increase in the WC content. The reasons for the same were not fully discussed.

Studies by Shin et al. [82] have demonstrated a significant improvement in the high temperature mechanical performance of W-3.6 wt% Re reinforced by HfC and ThO_2 particles as shown in Fig. 9. As the Fig. 9 shows, addition of 1 wt% of Thoria and 0.25 wt% HfC to W-3.6 wt%Re, leads to almost 2.5 times higher yield strength vis-à-vis W-3.6Re [83–85]. The superior performance of dispersion strengthened alloys is mainly due to the impediments to dislocation motion provided by the dispersion of hard particles, as shown in Fig. 10.

The improvement in creep behavior of W and its alloys brought about by the addition of dispersions was observed by King [86] and Yun [87]. King studied the creep behaviour of W and W-2 wt%ThO_2 prepared using the powder metallurgy route. Although the addition of the dispersion brought about an increase in the flow strength, the creep resistance, gaged by the minimum creep rates, of the W-2 wt% ThO2 was quite similar to that of W. King [86] who also observed that the creep data obtained from the W and W-2ThO_2 could not be described by conventional creep constitutive equations such as those proposed by the

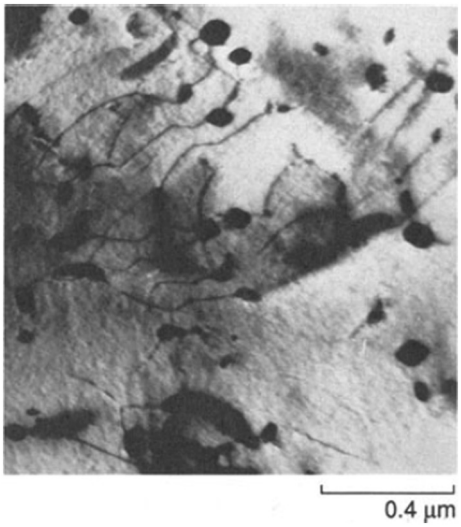

Fig. 10. Pinning down of dislocations by HfC particles in W-3.6Re-0.26HfC [82]

Bird-Mukherjee-Dorn equation or Robinson and Sherby [44]. Instead the data were better explained in plots of minimum creep rate against applied stress normalized by the flow strength of the material.

On the other hand, Yun [87] investigated the effect of ThO_2 and HfC addition on the creep behaviour of tungsten wires and found a definite enhancement in creep performance brought about the dispersions. Between HfC and ThO_2, the HfC dispersoids were found to provide a greater improvement in creep performance. Yun [87] also observed that potassium doped tungsten provided creep resistance similar to that of Thoria containing W samples. A threshold stress based model was adopted by Yun [87] to evaluate the creep data and a higher value of internal/threshold stress was observed in the HfC containing alloys compared to the K doped or ThO_2 dispersed alloy. The higher value of the internal stress indicates greater resistance to dislocation motion during creep deformation. Interestingly Yun [87] observed a superior creep performance of W-HfC system compared to the W-24Re-HfC system. This observation is similar to that of Witzke [81] who proposed that increased particle coarsening kinetics in the presence of Re is the cause of the poor creep resistance of W-24Re-HfC compared to the W-HfC system. All the systems investigated by Yun [87] i.e. potassium-doped tungsten, thoria-dispersed tungsten, HfC-dispersed W and HfC-dispersed W−24Re provided better creep performance compared to that of pure W.

In the study conducted by Galle et al. [63], the effect of La_2O_3 on the creep performance of W was evaluated. The higher creep resistance of W-La_2O_3 compared to the other alloys was attributed by Gallet et al. [63] to the impeding action of La_2O_3 dispersoids on the grain boundary migration, although as explained previously, under Harper-Dorn creep conditions the pinning down of dislocations by the La_2O_3 precipitates is a more reasonable explanation for improvement in creep performance.

3.4. Effect of grain shape on creep behaviour of tungsten and its alloys

Raj and Ashby [88] discussed the effect of grain shape on grain boundary sliding and diffusional creep. They noted that the strain rate attributable to volume and grain boundary diffusion and lattice diffusion varies strongly with grain shape even for small deviations from an equiaxed grain shape. Based on their calculations, Raj and Ashby found that diffusional creep is minimized by a large grain size with a large aspect ratio; the aspect ratio defined as the ratio of the height to the width of the grain.

The effect of grain shape was studied extensively by Wright [75] in 218 type doped tungsten (doped with potassium). The grain shape parameter was characterized using the grain aspect ratio (GAR). The grain aspect ratio is basically the ratio of the grain length to the grain width and can be varied by varying the time to recrystallization. An increase in the time to recrystallization brought about by low heating rates, yielded higher GAR values. Wright [75] determined the GAR of different microstructures and correlated the creep performance of doped tungsten to GAR values. Fig. 11 provides the time to rupture of various doped tungsten wires as a function of the GAR. As Fig. 11 illustrates, the time to rupture increases steeply with the GAR initially before hitting a plateau. Interestingly the activation energy of deformation was found to be 620 kJ/mol for a GAR value of 4 and was around 1600 kJ/mol for microstructures with GAR values of 19 and 35. The stress exponent for the low GAR microstructure was found to be 5.5 whereas it was 25 for the high GAR microstructures. Since very high stress exponent values are generally attributed to the presence of internal stresses resisting plastic deformation, Wright [75] proposed based on calculations that creep deformation in the high GAR microstructure was controlled by dislocation-dopant bubble interactions. A critical GAR value of 11 was suggested to differentiate between the low GAR and high GAR microstructures. There was a clear difference in the failure mode of the low and high GAR microstructures for creep tests carried out at high stresses (shown in Fig. 12 and 12b). For low GAR microstructures, the creep failure mode was intergranular in nature

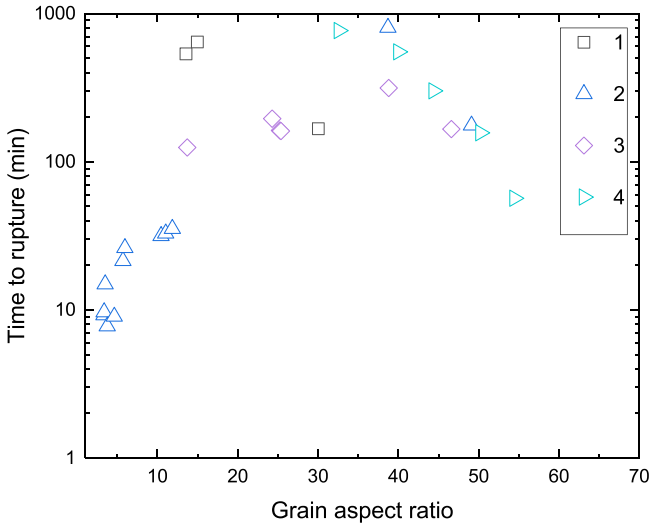

Fig. 11. Effect of grain aspect ratio on rupture life [75]

whereas the fracture pattern consisted of chiselled surfaces for the high GAR microstructures. The observation of chiselled fracture surface was taken as evidence for creep deformation controlled by the bulk of the grain with very low contribution whatsoever from the boundaries. The low contribution of grain boundaries to the creep deformation was attributed to the high degree of boundary locking prevalent in the high GAR microstructures, as a factor additional to that of dislocation-bubble interaction.

The dependence of strength on GAR has also been found in other systems [89,90]. Observations similar to that of Wright have also been found by Ignatiev et al. [91] in their study on tungsten nanocomposites. The creep performance of tungsten nanocomposites with oblong shaped grains was found to be superior to that of equiaxed grained samples, as shown in Fig. 13. The oblong shaped grains were achieved in uniaxially rolled foils whereas the equiaxed grains were achieved in the cross-rolled foils. The creep tests were carried out at 2470 K.

The grain shape effects have also been investigated by Tanoue [92]. Tanoue came up with three grain shape parameters, f1, f2 and f3. The f1 was described as characteristic of a complicated shape of grains accompanied with an increasing grain boundary area; f2 was described as important for torsional loads; and f3 was described as characteristic of the short range roughness of grain boundaries under conditions where f1 remains constant. It was found that increase in f1 and f2 leads to loss of high temperature creep resistance while f3 enhances creep resistance.Unlike Wright [75] and Ignatiev et al. [91], Tanoue [92] found that the creep rate decreases with increasing GAR < 30 and increases with increasing GAR > 30.

4. Conclusions

The creep behaviour of tungsten and its alloys will determine their suitability for high temperature applications such as plasma facing liners. Traditionally, tungsten is the choice of material for high temperature applications on account of its high melting point. However the applicability of tungsten is limited due to its poor ductility. The ductility of tungsten and its improvement strategies have remained a subject of intense investigations. Cold working, alloying with elements such as rhenium and grain morphology and grain size refinement have been identified as important factors for enhancing ductility and the effects of the same on creep behaviour have been discussed in this review. The effects can be summarized as follows

a. The addition of rhenium improves creep resistance albeit in lower concentration such as 5 wt%. The W−Re alloys with high quantities

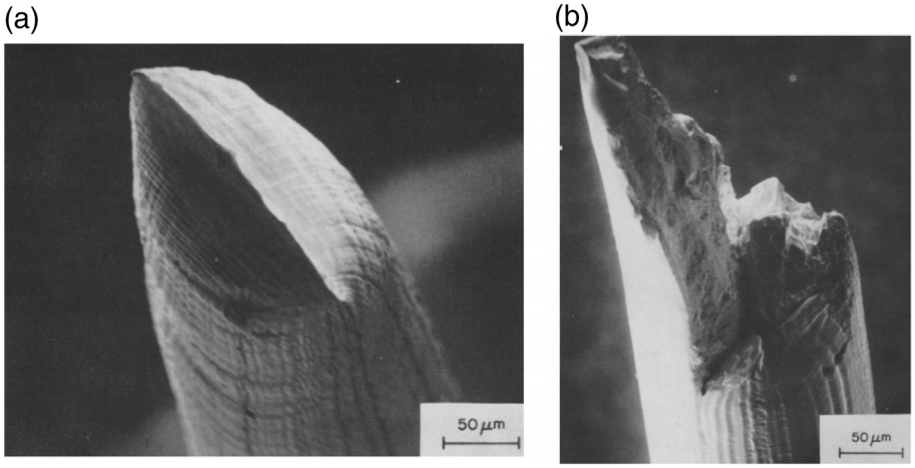

Fig. 12. a Intergranular fracture in tungsten with low "GAR" microstructure [75] (b) Transgranular fracture in tungsten with high "GAR" microstructure [75].

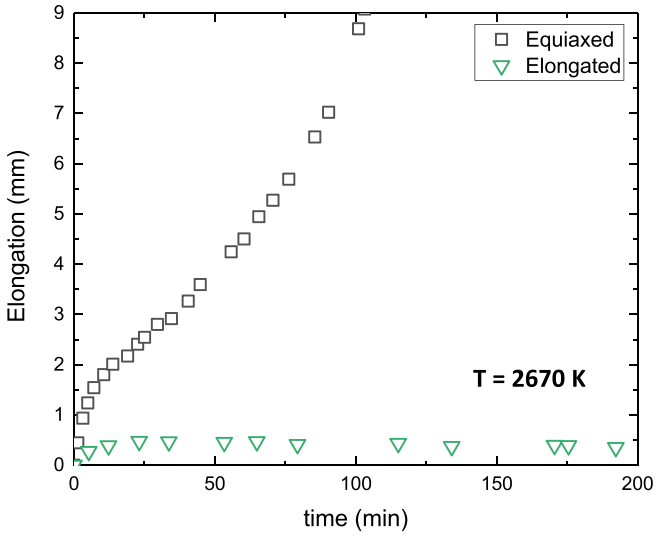

Fig. 13. Improved creep performance of tungsten nanocomposites with oblong shaped grains compared to tungsten nanocomposites with equiaxed grains [91].

of Re (~ 25 wt%) bear poorer creep resistance compared to the W–Re alloys with Re content of around 5 wt%.

b. The addition of dispersoids such as ThO_2, HfC or La_2O_3 improves the creep resistance of tungsten. The HfC was found to provide better enhancement in creep resistance compared to ThO_2 or La_2O_3.
c. Doping of tungsten with potassium improves its creep resistance. The potassium is known to encourage the creation of bubbles at grain boundaries that obstruct grain boundary motion leading to improvement in creep resistance.
d. The creep resistance of doped tungsten deteriorates in the presence of oxygen atmosphere even for very tiny oxygen levels.
e. The grain shape described by the grain aspect ratio (GAR) was found to have a definite impact on the creep behaviour of tungsten alloys. Higher GAR appears to enhance creep resistance.
f. Unlike conventional metals, the creep resistance of tungsten is apparently enhanced with grain size refinement.
g. It also appears that there is little difference in creep performance of powder metallurgy tungsten and arc/electron-beam-melted tungsten.

References

[1] S. Oghi, On the coarsening of non-sag tungsten filament wires, J. Phys. Soc. Jpn. 11 (1956) 593–598.
[2] T. Palacios, J. Reiser, J. Hoffman, M. Rieth, Microstructural and mechanical characterization of annealed tungsten and potassium doped tungsten foils, Int. J. Refract. Met. Hard Mater. 48 (2015) 145–149.
[3] I. Smid, H.D. Pacher, et al., Lifetime of be, CFC and W armoured ITER divertor plates, J. Nucl. Mater. 233–237 (1996) 701–707.
[4] J. Bakke, Y. Lei, Y. Xu, et al., Fluorine free tungsten films as low resistance liners for tungsten fill applications, 2016 IEEE International Interconnect Technology Conference / Advanced Metallization Conference (IITC/AMC), San Jose, CA, 2016, pp. 108-110, 2016.
[5] X. Liu, Y.Y. Lian, et al., Irradiation effects of hydrogen and helium plasma on different grades tungsten materials, Nuclear Mater. Energy 12 (2017) 1314–1318.
[6] www.iter.org.
[7] D.M. Duffy, Modeling plasma facing materials for fusion reactor, Mater. Today 12 (2009) 38–44.
[8] T. Kenmotsu, T. Ono, M. Wada, Effect of deuterium retention upon sputtering yield of tungsten by deuterons, J. Nucl. Mater. 415 (2011) S108–S111.
[9] 9. V. Philipps, Tungsten as material for plasma facing components in fusion devices, J. Nucl. Mater. 415 (2011) S2–S9.
[10] 10. K. Ohya, Progress in modelling erosion and redeposition on plasma facing materials, J. Nucl. Mater. 415 (2011) S10–S18.
[11] 11. A. Kallenbach, et al., Plasma surface interactions in impurity seeded plasmas, J. Nucl. Mater. 415 (2011) S19–S26.
[12] 12. Y. Ueda, J.W. Coenen, G.D. Temmerman, R.P. Doerner, J. Linke, V. Philipps, E. Tsitrone, Research status and issues of tungsten plasma facing materials for ITER and beyond, Fusion Engg. Des. 89 (2014) 901–906.
[13] 13. K. Wang, R.P. Doerner, M.J. Baldwin, C.M. Parish, Flux and fluence dependent helium plasma materials interaction in hot rolled and recrystallized tungsten, J. Nucl. Mater. 510 (2018) 80–92.
[14] 14. K. Wang, M.E. Bannister, F.W. Meyer, C.M. Parish, Effect of starting microstructure on helium-plasma materials interaction in tungsten, Acta Mater. 124 (2017) 556–567.
[15] B.G. Butler, J.D. Paramore, J.P. Ligda, et al., Mechanisms of deformation and ductility in tungsten- a review, Int. J. Refract. Met. Hard Mater. 75 (2018) 248–261.
[16] C. Ren, Z.Z. Fang, M. Koopman, B. Butler, J. Paramore, S. Middlemas, Methods for improving ductility of tungsten – a review, Int. J. Refract. Met. Hard Mater. 75 (2018) 170–183.
[17] Q. Wei, L. Kecskes, Effect of low-temperature rolling on the tensile behavior of commercially pure tungsten, Mater. Sci. Eng. A 491 (2008) 62–69.
[18] J. Reiser, J. Hoffmann, U. Jantsch, M. Kilmenkov, S. Bonk, C. Bonnekoh, M. Rieth, A. Hoffmann, T. Mrotzek, Ductilisation of tungsten (W): on the shift of the brittle-to-ductile transition (BDT) to lower temperatures through cold rolling, Int. J. Refract. Met. Hard Mater. 54 (2016) 351–369.
[19] Y. Song, D.S. Xu, R. Yang, D. Li, W.T. Wu, Z.X. Guo, Theoretical study of the effect of alloying additions on the strength and modulus of beta type bio titanium alloys, Mater. Sci. Eng. A 260 (1999) 269–274.
[20] T. Homma, N. Kunito, S. Kamado, Fabrication of extraordinary high-strength magnesium alloy by hot extrusion, Scr. Mater. 61 (2009) 644–647.
[21] G. Geach, J. Hughes, The Alloys of Rhenium with Molybdenum or with Tungsten and Having Good High Temperature Properties, Plansee Proceedings, Sintered High-Temperature and Corrosion-Resistant Materials: Papers Presented at the Second Plansee Seminar, 1955, pp. 245–253.
[22] A. Luo, D. Jacobson, K. Shin, Solution softening mechanism of iridium and rhenium in tungsten at room temperature, Int. J. Refract. Met. Hard Mater. 10 (1991) 107–114.
[23] J. Morris, Fracture-resistant dilute-solution ultralloys for space-power systems, Eng. Fract. Mech. 30 (1988) 609–626.
[24] R. Nygren, R. Raffray, D. Whyte, M. Urickson, M. Baldwin, L. Snead, Making tungsten work, J. Nucl. Mater. 417 (2011) 451–456.
[25] M. Faleschini, H. Kreuzer, D. Kiener, R. Pippan, Fracture toughness investigations of

tungsten alloys and SPD tungsten alloys, J. Nucl. Mater. 367–370 (2007) 800–805.
[26] L.J. Kecskes, K.C. Cho, R.J. Dowding, B.E. Schuster, R.Z. Valiev, Q. Wei, Grain size engineering of refractory bcc metals: top-down and bottom-up-application to tungsten, Mater. Sci. Eng. A 467 (2007) 33–43.
[27] K. Farrell, A.C. Schaffhauser, J.O. Steigler, Recrystallization, grain growth and ductile brittle transition in tungsten sheet, J. Less Common Met. 13 (1967) 141–155.
[28] D.B. Snow, The recrystallization of commercially pure and doped tungsten wire drawn to high strain, Metall. Trans. A. 10 (1979) 815–821.
[29] Robert E. Reed Hill, Physical metallurgy principles, 2nd edition, Van Nostrand, 1973.
[30] I. Wesemann, W. Spielmann, P. Heel, A. Hoffmann, Fracture strength and microstructure of ODS tungsten alloys, Int. J. Refract. Met. Hard Mater. 28 (2010) 687.
[31] Z.C. Chen, M.L. Zhou, T.Y. Zuo, Morphological evolution of second-phase particles during thermomechanical processing of W-La_2O_3 alloy, Scripta Mater. 43 (2000) 291.
[32] Xiao-Xin Zhang, Qing-Zhi Yan, Chun-Tian Yang, Tong-Nian Wang, Min Xia, Chang-Chun Ge, Recrystallization temperature of tungsten with different deformation degrees, Rare Metals 35 (2016) 566–570.
[33] M. Fukuda, T. Tabata, et al., Strain rate dependence of tensile properties of tungsten alloys for plasma facing components in fusion reactors, Fusion Eng. Des. 109-111 ((2016) 1674–1677.
[34] M.V. Aguirre, A. Martin, J.Y. Pastor, J. Llorca, M.A. Monge, R. Pareja, Mechanical properties of tungsten alloys with Y_2O_3 and titanium additions, J. Nucl. Mater. 417 (2011) 516–519.
[35] W. Klopp, W. Witzke, Mechanical Properties and Recrystallization Behavior of Electron-Beam-Melted Tungsten Compared with Arc-Melted Tungsten, National Aeronautics and Space Administration, NASA TN D-3232 (1966).
[36] W. Klopp, P. Raffo, Effects of Purity and Structure on Recrystallization, Grain Growth, Ductility, Tensile Strength and Creep Properties of Arc Melted Tungsten, National Aeronautics and Space Administration, (NASA TN D-2503), 1964.
[37] W. Klopp, W. Witzke, P. Raffo, Effects of Grain Size on the Tensile Stress and Creep Properties of Arc-Melted and Electron-Beam-Melted Tungsten, National Aeronautics and Space Administration, (NASA TM X-54756), 1964.
[38] M. Kassner, Taylor hardening in five power-law creep of metals and class-M alloys, Acta Mater. 52 (2004) 1–9.
[39] M. Kassner, Fundamentals of Creep in Metals and Alloys, Elsevier, 2009.
[40] S. Raj, *Power*-law and exponential creep in class-M materials: discrepancies in experimental observations and implications for creep modeling, Mater. Sci. Eng. A 322 (2002) 132–147.
[41] S. Raj, I. Iskovitz, A. Freed, Modeling the Role of Dislocation Substructure During Class-M and Exponential Creep, National Aeronautics and Space Administration, 1995 (NASA TM-106986).
[42] F. Nabarro, Do we have an acceptable model of power-law creep, Mater. Sci. Eng. A 387 (2004) 659–664.
[43] C. Barrett, O. Sherby, Influence of stacking fault energy on high temperature creep of pure metals, Trans. Metall. Soc. AIME 233 (1965) 1116–1119.
[44] S. Robinson, O. Sherby, Mechanical behavior of polycrystalline tungsten at elevated temperature, Acta Metall. 17 (1969) 109–125.
[45] H. Luthy, A. Miller, O. Sherby, The stress and temperature dependence of steady state flow stress at intermediate temperatures for pure aluminum, Acta Metall. 28 (1980) 169–178.
[46] G. King, H. Sell, The effect of thoria on the elevated-temperature tensile properties of recrystallized high purity tungsten, Trans. Metall. Soc. AIME 82 (5) (1965) 1104–1113.
[47] W. Green, Short time creep rupture behavior of tungsten at 2250 to 2800 C, Trans. Metall. Soc. AIME 215 (1959) 1058–1161.
[48] B. Harris, E. Ellison, Creep and tensile properties of heavily drawn tungsten wire, Trans. Of ASM 59 (1966) 744–754.
[49] J. Conway, P. Flagella, Physical and mechanical properties of reactor materials, Seventh Annual Report, AEC Fuels and Materials Development Program, 1968.
[50] R. Pawel, T. Lundy, Tracer diffusion in tungsten, Acta Metall. 17 (1969) 979–988.
[51] G. Neumann, C. Tujin, Self Diffusion in Pure Metals, Elseviar, 2009.
[52] R. Andelin, J. Knight, D. Khan, Diffusion of tungsten and rhenium tracers in tungsten, Trans. Metall. Soc. AIME 233 (1965) 19–24.
[53] J. Mundy, S. Rothman, N. Lam, H. Hoff, L. Nowicki, Self diffusion in tungsten, Phys. Rev. B 18 (1978) 6566–6571.
[54] P. Gordon, R. Vandemeer, The mechanisms of boundary migration in recrystallization, Trans. Metall. Soc. AIME 224 (1962) 917–928.
[55] K. Aust, J. Rutter, Temperature dependence of grain boundary migration in high purity Lead containing small additions of tin, Trans. Metall. Soc. AIME 215 (5) (1959) 820–831.
[56] H.J. Frost, M.F. Ashby, Deformation Mechanism Maps, the Plasticity and Creep of Metals and Ceramics, Permagon Press, 1983.
[57] E. Sutherland, W. Klopp, Observations of Properties of Sintered Wrought Tungsten Sheet at Very High Temperatures, National Aeronautics and Space Administration, 1963 (NASA TN D-1310).
[58] R.L. Coble, Diffusion models for hot pressing with surface energy and pressure effects as driving forces, J. Appl. Phys. 41 (12) (1970) 4798–4807.
[59] M.F. Ashby, A first report on deformation-mechanism maps, Acta Metall. 20 (1972) 887–897.
[60] M.F. Ashby, A first report on sintering diagrams, Acta Metall. 22 (1972) 275–289.
[61] R.M. German, Sintering Theory and Practice, Wiley, New York, 1996.
[62] Joseph Davis (Ed.), Alloying: Understanding the Basics, ASM International, Materials Park, Ohio, 2001.
[63] D. Gallet, J. Dhers, R. Levoy, P. Polcik, Creep laws for refractory tungsten alloys between 900 C and 1100 C at low stress, in: G. Kneringer, P. Rodhammer, H. Wildner (Eds.), 15th Int. Plansee Seminar, vol. 1, 2001.
[64] J. Harper, J.E. Dorn, Viscous creep of aluminium near its melting point, Acta Metall. 5 (1957) 654–665.
[65] F.R.N. Nabarro, Report of Conf. On Strength of Solids, Physics Society, London, 1948, p. 75.
[66] C. Herring, Diffusional viscosity of a polycrystalline solid, J. Appl. Phys. 21 (1950) 437.
[67] R.L. Coble, A model for boundary diffusion controlled creep in polycrystalline materials, J. Appl. Phys. 34 (1963) 1679.
[68] P.L. Raffo, W.D. Klopp, Influence of B Additions on Physical and Mechanical Properties of Arc-Melted W and W-1%ta Alloy (NASA TN D-3247), Feb, (1966).
[69] K.I. Portnoi, V.M. Romashov, Yu.V. Levinskii, I.V. Romanovich, Phase diagram of the system tungsten-boron, Sov. Powder Metall. Met. Ceram. 6 (1967) 398–402.
[70] M. Ekman, K. Persson, G. Grimvall, Phase diagram and lattice instability in tungsten-rhenium alloys, J. Nucl. Mater. 278 (2000) 273–276.
[71] W.D. Klopp, W.R. Witzke, P.L. Raffo, Mechanical Properties of Dilute Tungsten-Rhenium Alloys, NASA Technical Note, NASA TN D-3483 (1966).
[72] R.P. Vandervoort, The creep behaviour of W-5Re, Metall. Trans. A. 1 (1970) 857–864.
[73] K.L. Murty, Transitional creep mechanisms in Al-5Mg at high stresses, Scripta Met. 7 (1973) 899–903.
[74] H.P. Gao, R.H. Zee, Effects of rhenium on creep resistance in tungsten alloys, J. Mater. Sci. Lett. 20 (2001) 885–887.
[75] P.K. Wright, The high temperature creep behaviour of doped tungsten wire, Metall. Trans. A. 9A (1978) 955–963.
[76] P. Schade, Potassium bubble growth in tungsten, Int. J. Refract. Met. Hard Mater. 16 (1998) 77–87.
[77] K. Tanoue, R. Ijichi, Effect of potassium concentration on threshold stress during creep at high temperatures in doped tungsten fine wires, J. Japan Inst. Metals 66 (2) (2002) 75–80.
[78] Vladica Nikolić, Johann Riesch, Reinhard Pippan, The effect of heat treatments on pure and potassium doped drawn tungsten wires: part I: microstructural characterization, Mater. Sci. Engg. A 737 (2018) 422–433.
[79] D. Terentyev, J. Riesch, S. Lebediev, T. Khvan, A. Dubinko, A. Bakaeva, Strength and deformation mechanism of tungsten wires exposed to high temperature annealing: impact of potassium doping, Int. J. Refract. Met. Hard Mater. 76 (2018) 226–233.
[80] G. Zilberstein, Creep properties of non sag tungsten recrystallized in stagnant oxygen doped argon, Int. J. Refract. Met. Hard Mater. 16 (1998) 71–75.
[81] W. Witzke, Composition Effects on the Mechanical Properties of Tungsten-Rhenium-Hafnium-Carbon Alloys, NASA Technical Note, NASA TN D-7210 (1973).
[82] K.S. Shin, A. Luo, B.-L. Chen, D.L. Jacobson, High temperature properties of particle strengthened W-re, JOM 12 (1990) 12. August.
[83] A. Luo, D. L. Jacobson, K.S. Shin, High temperature tensile properties of a W-3.6Re-1 ThO_2 alloys, Mater. Sci. Eng. A 148 (1991) 219–229.
[84] A. Luo, D.L. Jacobson, K.S. Shin, High-Temperature Tensile Properties of W-Base Alloys, Paper Presented at the 118th TMS Annual Meeting, Las Vegas, Nevada, March (1989).
[85] B.L. Chen, High Temperature Creep Behaviour of Second Phase Particle Strengthened Tungsten-Rhenium Alloys (PhD thesis), Arizona State University, 1990.
[86] G.W. King, The stress dependence of high temperature creep of tungsten and a tungsten – 2 weight percent ThO_2 alloy, Metall. Trans. A. 3 (1972) 941–945.
[87] H.M. Yun, Effect of composition and microstructure on the creep and stress-rupture behaviour of tungsten alloy wires at 1366-1500 K, Mater. Sci. Eng. 165A (1993) 65074.
[88] R. Raj, M.F. Ashby, On grain boundary sliding and diffusional creep, Metall. Trans. A. 2 (1971) 1113–1127.
[89] B.A. Wilcox, A.H. Clauer, The role of grain shape and size in strengthening of dispersion hardened Ni alloys, Acta Metall. 20 (1972) 743–757.
[90] J.J. Petrovic, L.J. Ebert, Elevated temperature deformation of TD-nickel, Metall. Trans. A. 4 (1973) 1301–1308.
[91] D.N. Ignatiev, A.A. Pavlov, E.S. Solntseva, M.L. Taubin, A.A. Yaskolko, Thermal stability and high-temperature deformation of tungsten nanocomposite, IOP Conf. Ser. 130 (2016) 012014.
[92] K. Tanoue, Grain shape parameters for high temperature creep resistance in powder metallurgy tungsten fine wires, Metall. Mater. Trans. A 29A (1998) 519–526.